Polymer 103 (2016) 180–188

Contents lists available at ScienceDirect

Polymer

journal homepage: www.elsevier.com/locate/polymer

Self-healing of nanofiber-based composites in the course of stretching

Min Wook Lee [a], Soumyadip Sett [a], Sam S. Yoon [b, **], Alexander L. Yarin [a, b, *]

[a] Department of Mechanical and Industrial Engineering, University of Illinois at Chicago, Illinois 60607-7022, USA
[b] School of Mechanical Engineering, Korea University, Seoul 136-713, Republic of Korea

ARTICLE INFO

Article history:
Received 17 July 2016
Received in revised form
2 September 2016
Accepted 12 September 2016
Available online 13 September 2016

Keywords:
Self-healing
Nanofiber
Composite

ABSTRACT

Here we aim to elucidate the self-healing mechanisms in composites with embedded solution-blown nanofibers containing separate reservoirs of epoxy resin and hardener in their cores. In tensile tests of such composite materials with the resin- and hardener-containing solution-blown nanofibers embedded in a polymer matrix, it is shown that the fibers can be ruptured by stretching, thereby releasing the epoxy resin and hardener. Given a resting (or holding) period of 1–2 h, such materials can experience a restoration or even enhancement of stiffness in subsequent stretching, thereby displaying self-healing properties. In two model macroscopic experiments with a single crack tip, conducted in the Appendix with the aim to elucidate the self-healing mechanism, the epoxy resin and hardener released into the tip are shown to react with each other, resulting in a cured and hardened epoxy that heals the crack tip.

1. Introduction

Self-healing in nature is a complex and fascinating phenomenon [1]. It occurs repeatedly on scratched skin and broken bones, unless the damage to the body is too severe. The element crucial to successful self-healing in mammals is the vascular system. When a wound such as a skin scratch occurs, it starts bleeding. This bleeding delivers healing materials to the damaged site through the blood vessels of the organism. This process works rapidly to form a crust at the bleeding zone, stopping the bleeding and preventing further damage. This kind of self-healing system is also desirable in engineering materials [2–5]. Micro- and nanofibers or tubes can serve as substitutes for blood vessels in self-healing engineering materials. Healing agents, such as resin monomers and curing species or epoxy resin and hardeners, can be delivered through these fibers or tubes like blood. The healing agents stored in the fibers are released from the ruptured fibers, become polymerized or solidified, and thereby heal the broken fiber ends. After this engineered curing process, the damaged site can be healed, accompanied by a partial or complete recovery or even an enhancement of the macroscopic mechanical properties, such as stiffness and strength [3,5–7].

If damage is associated with crack propagation, self-healing may prevent or impede the crack growth to the point of catastrophic failure. A special type of crack propagation along ply surfaces in composite materials can cause delamination and failure of the composites. Many useful, efficient, and lightweight composite materials are vulnerable to the growth of fatigue cracks and the resulting delamination [5,8,9]. Moreover, it is almost impossible to discover and repair such flaws within the composites. Even very small cracks can start growing rapidly, causing failure of the entire structure [10]. The application of such composite materials in high-risk structures requires backup for safety.

Self-healing of composite materials has been demonstrated for material damage caused by bending [3,5], stretching [11,12], and delamination [13,14]. The stiffness could be recovered, either fully or partially, from a certain level of material damage by curing of the released healing agents at the damaged sites. In addition, surface scratches on coatings that protected metal substrates could be patched to avoid corrosion problems. The anti-corrosive coatings containing healing agents were successfully self-healed, preventing corrosion of the underlying metal [15–17].

In the past, self-healing of the pre-notched cracks in strips under static tension was demonstrated [18]. In the present work, the growth and self-healing of pre-notched cracks in composite strips subjected to increasing tensile stresses are investigated.

* Corresponding author. Department of Mechanical and Industrial Engineering, University of Illinois at Chicago, Illinois 60607-7022, USA.
** Corresponding author.
E-mail addresses: ayarin@uic.edu (A.L. Yarin), skyoon@korea.ac.kr (S.S. Yoon).

http://dx.doi.org/10.1016/j.polymer.2016.09.037
0032-3861/

2. Experimental

2.1. Materials

Two polymers, poly(vinylidene fluoride) (PVDF, $M_w \approx 180$ kDa) and poly(ethylene oxide) (PEO, $M_w = 200$ kDa), and two solvents, dimethylformamide (DMF) and acetone, were purchased from Sigma-Aldrich. A two-part commercial epoxy kit, ClearWeld (JB WELD), was purchased at a local hardware shop. The two components of the epoxy, the resin and hardener, have a 1:1 mixing ratio. When mixed, the resin sets in 5 min and reaches a fully cured state in 1 h at room temperature. Neither the resin nor the hardener of the epoxy is volatile in nature. Polydimethylsiloxane (PDMS) was obtained from Ellsworth Adhesives.

2.2. Solution preparation

A 2:3 (w/w) acetone/DMF mixture was used as the solvent for PVDF and a 21% (w/w) PVDF solution was prepared. PEO was dissolved in a 2:10 (w/w) acetone/DMF mixed solvent to prepare a 4% (w/w) PEO solution. Core-shell fibers were developed with the healing agent components (the epoxy resin and hardener) encased in the cores separately, within polymeric shells. The shell polymer solution was prepared by mixing 5 g of the above-mentioned PVDF solution with 2 g of the above-mentioned PEO solution. Since both the epoxy resin and the hardener are about 8 and 50 times more viscous than water, respectively, they were diluted in DMF (8:5 w/w) to lower their viscosities and create suitable solutes for the solutions used to form the fiber cores. Some core-shell fibers were formed with the epoxy resin in the core, while the others contained the hardener in the core. Both types of core-shell fibers were deposited in a single interwoven layer, as described in section 2.3.

2.3. Dual coaxial solution-blowing

The dual coaxial solution-blowing technique used for nanofiber generation is explained in detail in our previous work [18], which addressed the static tensile tests used to evaluate the self-healing of cracks in composites subjected to static loading. In brief, to encapsulate either the epoxy resin or its hardener within the fibers, core DMF-diluted solutions of either of these materials were used. The PVDF/PEO mixed solution was used as the shell solution for both types of fibers. The core and shell solutions were supplied separately to a core-shell needle. The shell flow rate was 5 mL/h and the core flow rate was 1 mL/h in both cases. As described in detail in our previous works [14,18], the core-shell needle was encased in a coaxial air nozzle, which issued a high-speed air jet at a pressure of 40–50 psi. Two parallel sets of core-shell fibers with either the epoxy resin or the hardener in the core were solution-blown simultaneously from two core-shell nozzles in coaxial air nozzles. The core-shell epoxy resin-PVDF/PEO and hardener-PVDF/PEO nanofibers were collected on a rotating drum of 20 cm in diameter and 13 cm in width. The mesh covering the drum was vacuumized from the inside, which facilitated nanofiber collection on the drum. The simultaneous solution blowing of this interwoven layer of the two types of core-shell fibers was conducted for 30 min. For comparison with the self-healing fibers, monolithic PVDF/PEO fibers containing no epoxy or hardener were also solution-blown.

2.4. Sample preparation

The solution-blown nanofiber mats with and without epoxy were cut into 20 mm × 60 mm strips. Separately, the PDMS resin and curing agent were mixed in a 10:1 ratio and the cut fiber strips were cast into the premixed PDMS. The PDMS matrices with the encased fiber strips were allowed to cure in open air at room temperature for 24–48 h. The thickness of each composite sample prepared in this way was then measured at three different locations, with average values reported below. The uniformity of composites is not under a full control because the nanofiber mat is not distributed uniformly inside the PDMS matrix. The thicknesses of the as-spun nanofiber mats are about 0.11–0.12 mm, while the thicknesses of the composite samples with and without epoxy resin and hardener in the nanofiber cores were about 0.53–0.67 mm. The embedded nanofiber mat in a similar PDMS matrix is shown in Fig. 2 in Ref. [18] (the image is not shown here).

2.5. Dynamic tensile test with crack growth

The PDMS-fiber composite samples fabricated as described in the previous subsection were used for tensile tests. However, unlike the static tests described in our previous work [18], here the tensile stress was increased over time, i.e., the loading was dynamic. In these dynamic tensile tests with crack growth, the upper and lower ends of the composite samples were tightly gripped by the clamps of an Instron machine (model 5942) with a 100 N load cell. The initial gap between the upper and lower clamps was 20 mm in all the experiments. An initial horizontal incision was introduced in the middle of the sample, as shown in the magnified image of the sample in Fig. 1. The samples were then uniaxially stretched at the strain rate of either $\dot{\varepsilon} = 0.05$ mm/min (= 3 mm/h) or $\dot{\varepsilon} = 0.025$ mm/min (= 1.5 mm/h) by the motion of the upper grip. The lower grip remained stationary. This initial stretching was done until the elongation reached $\ell = 3$ mm in addition to the initial gap of 20 mm (for 1 h or 2 h, depending on the stretching rate) or $\ell = 1.5$ mm in addition to the 20-mm initial length (for 0.5 h or 1 h, depending on the stretching rate).

The stretching was then stopped and the samples were maintained in a stationary position with fixed grips for 1 or 2 h. Since the epoxy resin used in the fibers has a hardening time of 1 h, this waiting time was considered sufficient for crack healing to occur in the samples containing self-healing nanofibers.

At the end of the waiting time, the second stage of stretching was begun. The sample stretching was continued at the initial stretching rate until sample failure by the initial central crack reaching a catastrophic size. The stress-strain curve for the entire experiment, including both the initial and second stages of stretching, was measured by the Instron machine. In parallel, a digital camera (Nikon D3200) was used to photograph the sample with a focus on the propagating crack. Photographs were obtained at regular intervals of 1 min until the sample failed. All the experiments were repeated 2–3 times at least to corroborate the results.

2.6. Image processing

The time-dependent lengths of the cracks were measured using processed captured images in MATLAB. The lighting was maintained to create a distinct contrast between the composite sample surface and the crack in the center. Using the grayscale image in MATLAB, a proper threshold was set so that the entire image could be converted to black and white. The crack in the middle of the sample was black while the surrounding composite material was uniformly white. The crack length was then measured by counting the number of black pixels in the horizontal direction.

3. Dynamic tensile test with crack growth in composites with embedded self-healing nanofibers: results and discussion

The solution blown nanofibers form randomly oriented

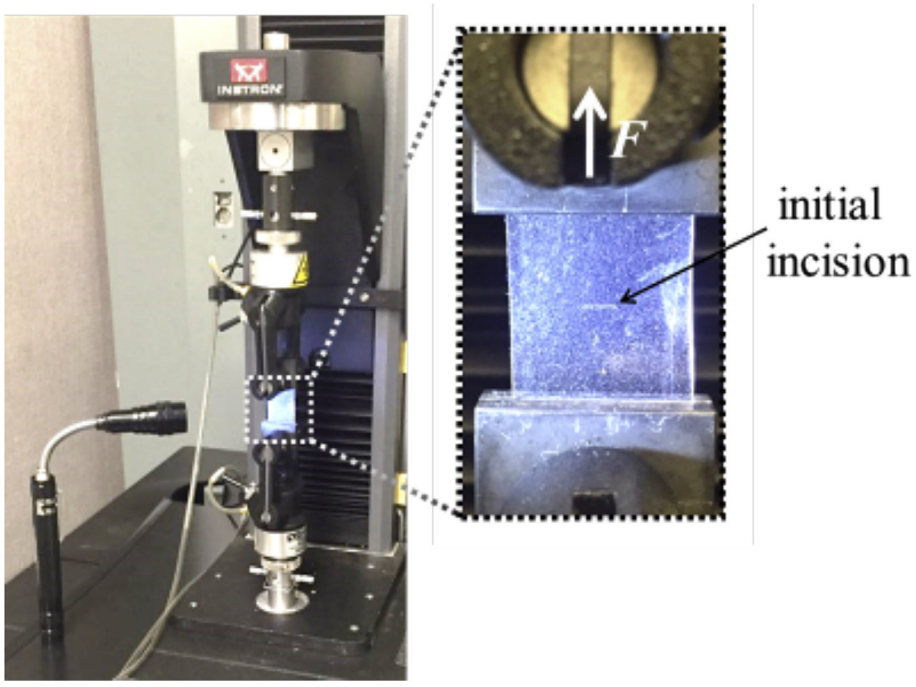

Fig. 1. Dynamic tensile tests with crack growth for PDMS-fiber composites at fixed strain rates using Instron machine. The magnified image on the right shows the loaded sample with the initial pre-notched incision prior to the beginning of stretching.

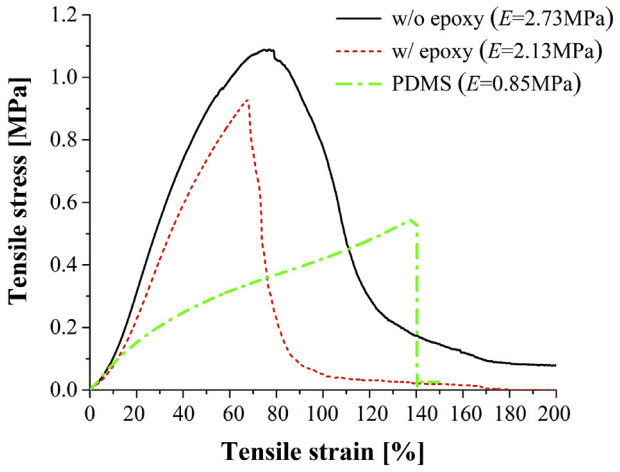

Fig. 2. Stress-strain curve of as-spun PVDF/PEO nanofiber mat with (w/) and without (w/o) epoxy resin and hardener and the stress-strain curve of neat PDMS.

nonwoven. The contents of nanofibers in the PDMS matrices in the composites studied in the present work was about 3.21 wt% (the core-shell nanofibers with epoxy resin and hardener in the cores) and about 2.68 wt% (the nanofibers without healing agents). The Young's moduli of PVDF/PEO nanofiber mats with and without epoxy and hardener were 2.13, and 2.73 MPa, respectively [18]. In comparison with pure PDMS matrix (with E = 0.85 MPa), the PVDF/PEO nanofiber mats are stiffer and stronger by a factor of about 2.5–3.2 (see Fig. 2). It should be emphasized that stretching of nanofiber mats, as usual, is accompanied by the fiber re-orientation predominantly in the stretching direction. Debonding and fiber fracture are minor up to the strains of $\varepsilon = 7.5$ or 15% explored in the experiments related to self-healing discussed in Figs. 3 and 4, since the slope of the stress-strain curves there practically do not change.

The stress-strain curves, along with the time-dependent crack length, for samples containing nanofibers with and without epoxy components subjected to tensile tests at the constant stretching rate of 3 mm/h are shown in Fig. 3. In all cases, (#-1) corresponds to samples with PVDF/PEO fibers alone, while (#-2) corresponds to samples containing fibers with epoxy components. Initially, the composite samples were stretched for 1 h (3 mm, 15% strain) and held for another 1 h before further stretching (Figs. 3a-1 and 3a-2). By the nature of the epoxy, the 1 h holding time was expected to be sufficient for the composite samples with epoxy-containing nanofibers to heal. In general, the composites failed at ~25% strain. Hence, 1 h of stretching causing 15% strain is expected to provide moderate damage to the samples, large enough for the composites with epoxy to heal but too small for an irrepairable damage to happen. Moreover, this moderate damage ensures that only the nanofibers within the PDMS matrix would be ruptured by stretching, maintaining the intact external PDMS in the reversible region of elastic deformation. It should be emphasized that the encased nanofibers are stiffer and stronger than the PDMS matrix (cf. Fig. 2), so the experiments reached the level of fiber damaging, which alone could trigger the observed self-healing effects.

For the next set of tests, the initial stretching time was reduced to 30 min (1.5 mm, 7.5% strain), thereby inflicting less damage on the samples (Figs. 3b-1 and 3b-2). The holding time was the same, i.e. 1 h.

For the third set of tests, the initial stretching time was 1 h (3 mm, 15% strain), identical to the first case. However, the holding time was increased from 1 h to 2 h, to elucidate the effect of the holding time on the reaction of the resin and hardener, solidification of the epoxy, and self-healing behavior of the composites.

For the first set of tests, the stress-strain curves for the composites containing PVDF/PEO nanofibers alone before (in black in Fig. 3) and after (in red in Fig. 3) the holding period have nearly equal slopes, with a decrease of ~0.3% recorded after holding,

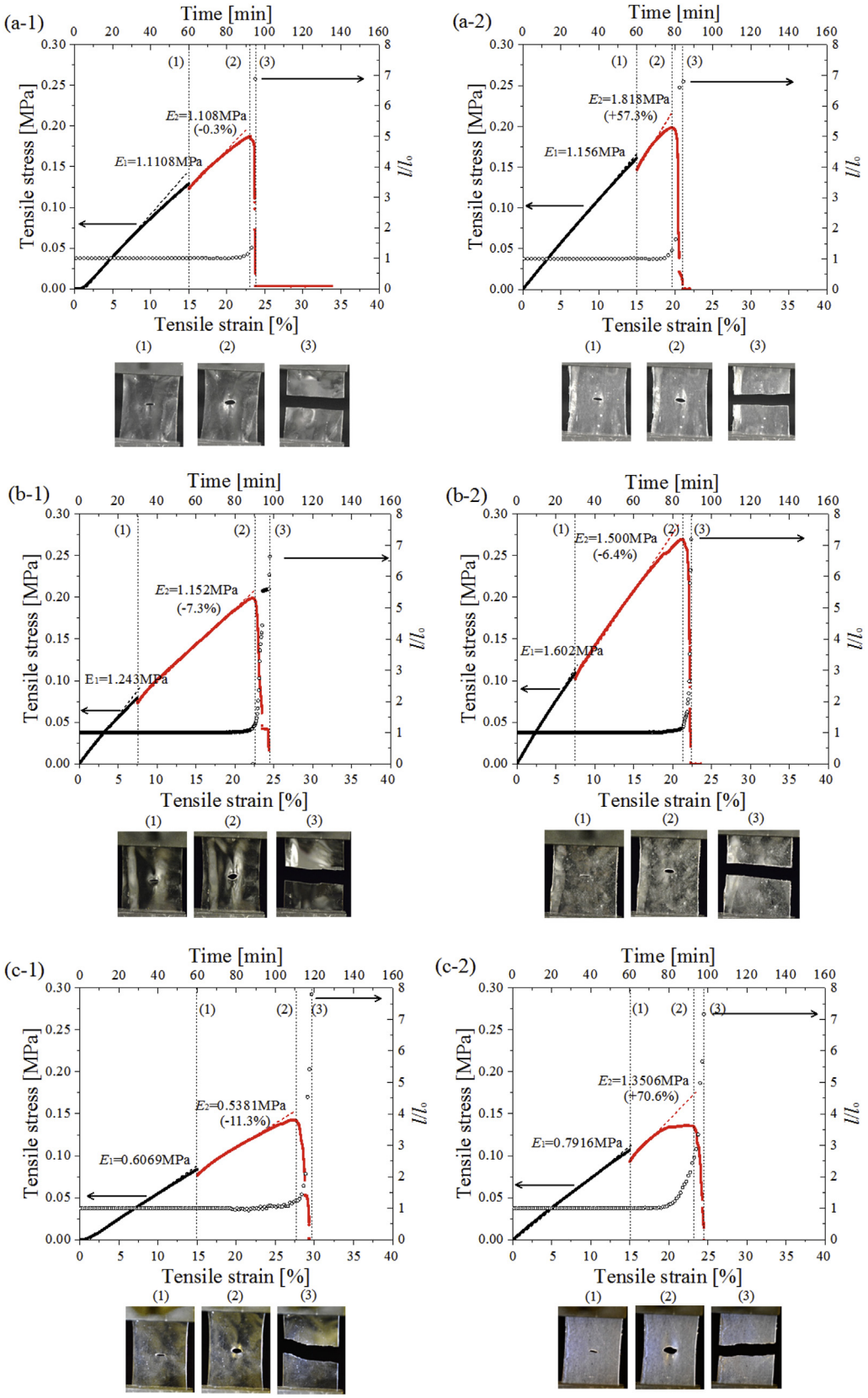

Fig. 3. Stress-strain curves and normalized crack lengths (l/l_o) in tensile tests of composites without and with epoxy components encapsulated in the embedded nanofibers at the strain rate of 3 mm/h (= 0.05 mm/min). Panels (a): stretching length 3 mm, holding period 1 h. Panels (b): stretching length 1.5 mm, holding period 1 h. Panels (c): stretching length 3 mm, holding period 2 h. The suffix −1 corresponds to samples with PVDF/PEO fibers alone and the suffix −2 corresponds to samples containing nanofibers with epoxy components. In each panel, the black and red bold lines correspond to the initial and post-holding stretching stages, respectively. The black open circles indicate the dimensionless crack length versus time. The photographs of the composite samples labelled (1), (2), and (3) underneath each stress-strain curve depict the samples at the end of the holding period, the point of the maximum stress, and complete failure. (For interpretation of the references to colour in this figure legend, the reader is referred to the web version of this article.)

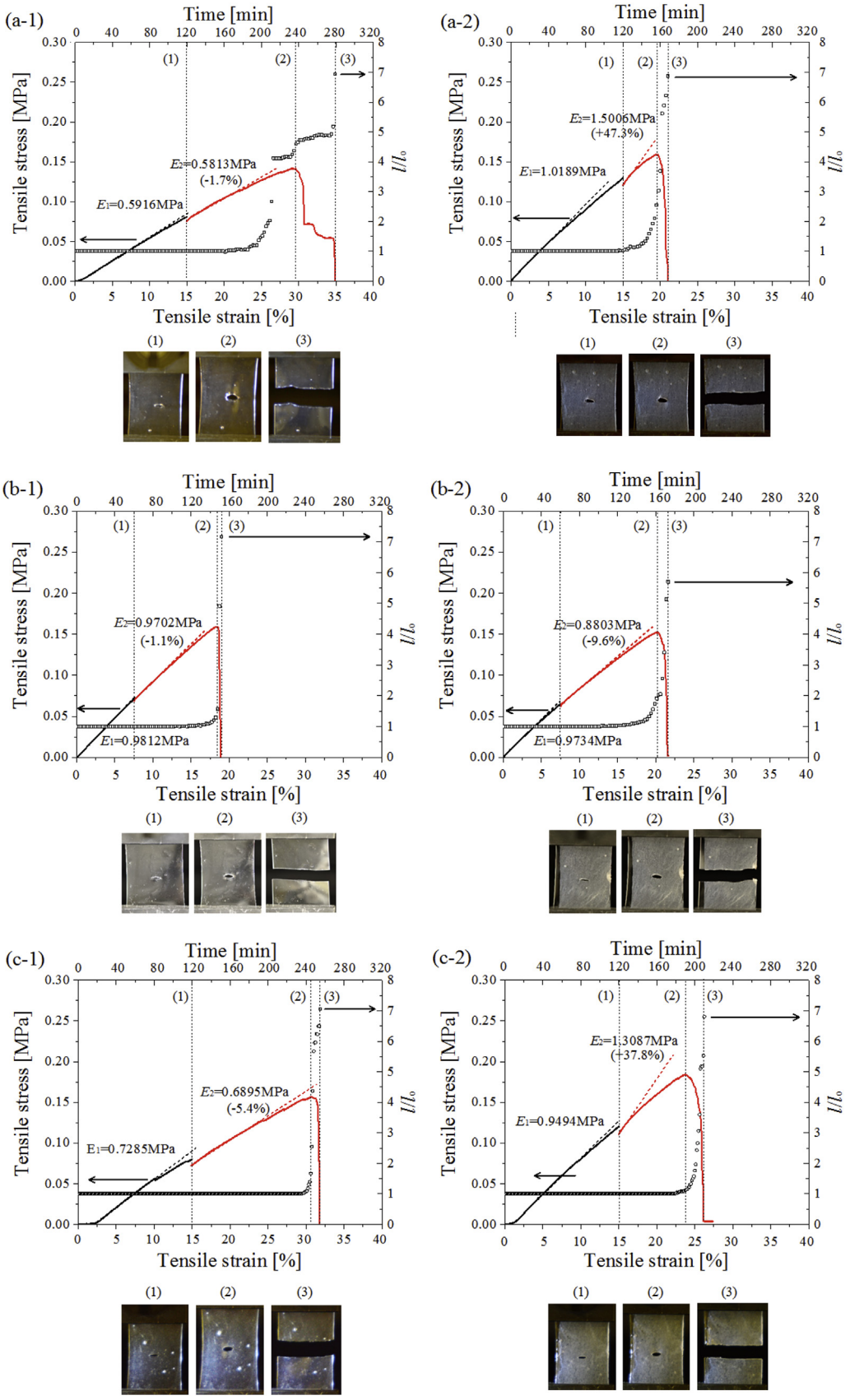

Fig. 4. Stress-strain curves and normalized crack lengths (l/l_o) in tensile tests of composites without and with epoxy components at the strain rate of 1.5 mm/h (= 0.025 mm/min). Panels (a): stretching length 3 mm, holding period 1 h. Panels (b): stretching length 1.5 mm, holding period 1 h. Panels (c): stretching length 3 mm, holding time 2 h. The suffix −1 corresponds to samples with PVDF/PEO fibers alone and the suffix −2 corresponds to samples containing fibers with epoxy components. In each panel, the black and red bold lines correspond to the initial and post-holding stages of stretching, respectively. The black open circles correspond to the dimensionless crack lengths versus time. The photographs of the composite samples labelled (1), (2), and (3) underneath the stress-strain curves depict the end of the holding period, the point of the maximum stress, and complete failure. (For interpretation of the references to colour in this figure legend, the reader is referred to the web version of this article.)

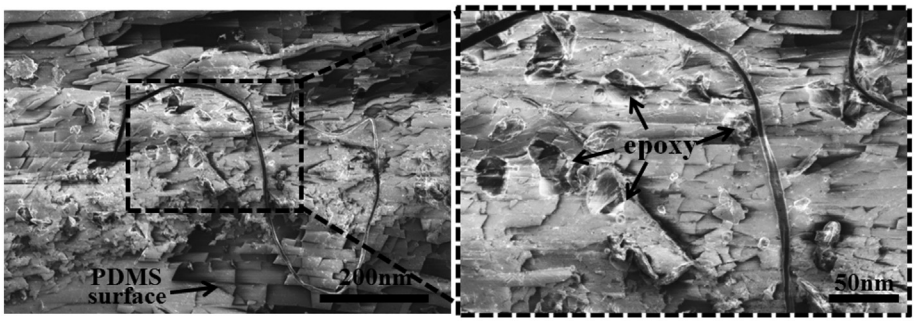

Fig. 5. SEM micro-image of the fractured surface of a composite sample containing self-healing nanofibers.

indicating that no increase in stiffness occurs during the 1-h holding period (Fig. 3a-1). Since these nanofibers have no self-healing material, the holding period is expected to neither affect the stiffness nor lead to healing of the composite. Meanwhile, the composites with nanofibers containing epoxy components show a remarkable enhancement in stiffness after the holding period (Fig. 3a-2). This indicates that the 1-h holding period is sufficient for the reaction between the two components, the epoxy and the hardener of the cured epoxy. The Young's modulus for these samples dramatically increased by 57.3% from $E_1 = 1.156$ MPa to $E_2 = 1.818$ MPa at the post-holding stretching stage, implying a significant self-healing of the composites.

For the second set of tests, in which the samples were initially stretched for a shorter time interval (30 min instead of 1 h), no increase in stiffness was observed, even for the composites containing nanofibers with epoxy components (Fig. 3b-2). This indicates that the damage caused by 7.5% strain was insufficient to cause nanofiber rupture and the release of the self-healing materials. Therefore, no healing is observed. The stiffness and Young's moduli of these composites, even those containing nanofibers with the epoxy components, are constant before and after the holding period.

For the third set of tests, a strain of 15% was applied to the samples before the holding period. The holding time for these tests was increased to 2 h. As expected, the composites with PVDF/PEO nanofibers alone show no increase in stiffness during the stretching after the holding period (Fig. 3c-1). The stiffness is instead decreased by 11.3%. Meanwhile, the composites containing nanofibers with the epoxy components display a remarkable increase in stiffness when the samples are stretched after the 2-h holding period, with the Young's modulus increasing by ~70.6% from $E_1 = 0.7916$ MPa to $E_2 = 1.3506$ MPa (Fig. 3c-2). The opposite trends in stiffness observed for the samples with nanofibers with and without the epoxy components demonstrate that the latter samples are damaged by stretching and inherently lose mechanical properties, thereby causing a reduction in stiffness. However, composites with the epoxy components are capable of self-healing during the healing period of 2 h, causing the stiffness to increase. The increase in stiffness for the epoxy-containing composites over the 2-h holding time is more pronounced than that observed over the shorter 1-h holding time, indicating that longer holding times cause greater healing in the samples. Thus, in both cases when the self-healing samples were moderately damaged, the epoxy cured the damaged sites, which increased the composite stiffness.

The crack length measurements over time (open black circles in Fig. 3) reveal that the crack length remains nearly constant throughout the tensile tests, except during the final stages when the tensile stress is maximized. This is evident from the fact that the normalized crack length l/l_0 (where l_0 is the initial crack length) remains equal to 1 for most of the tensile test. This, however, does not mean that the cracks do not grow and no damage is done. The sub-critical crack growth is possible, albeit visually practically undetectable [18–20]. As the stress approaches the critical maximum value (the second vertical dashed line from the left in Fig. 3), the crack starts to propagate rapidly, and the composite sample fails within a few minutes. The sudden increase in the crack length is accompanied by the rapid decrease in the tensile stress to zero (the third vertical dashed line from the left in Fig. 3), indicating the catastrophic failure of the composite samples.

To study the effect of the rate of stretching on self-healing of the composites, tensile tests were also conducted at the lower strain rate of 0.025 mm/min (0.15 mm/h) for different initial stretching times and different holding periods. The results were similar to those in Fig. 3. Namely, the composites containing only PVDF/PEO fibers show, as expected, no enhancement in stiffness after the holding period (Figs. 4a-1, 4b-1, and 4c-1) irrespective of the holding position or time. A significant increase in stiffness is observed for the composites containing fibers with epoxy components for the initial stretching of 3 mm (2 h of stretching up to 15% strain). The following 1 h of holding results in a ~47.3% increase in the Young's modulus (Fig. 4a-2), whereas a 2-h holding period causes a ~37.8% increase (Fig. 4c-2). Unlike the case of the higher strain rate shown in Fig. 3, in this case, the longer holding period does not cause further increases in the stiffness. This could be because the lower rate of stretching causes less damage to the epoxy-component-containing nanofibers compared to the previous case corresponding to Fig. 3.

Definitely curing may have happened at the initial crack, as well as at any crack but it takes time on the scale of hours. Therefore, the initial incision can release the epoxy resin and hardener but cure could not happen immediately, as well as during the stretching up to the strains of $\varepsilon = 7.5$ or 15% corresponding to positions (1) in Figs. 3 and 4. During this first stage of stretching the slope of the stress-strain curves did not visibly changed, which corroborates the fact that no cure happened during these relatively short periods of time, even though the epoxy resin and hardener have been already released from the initial and growing cracks. Only after a rest (holding) period of $t = 1–2$ h which is sufficient to the cure reaction to proceed, at the second stretching stage after the holding period, we observed an increase in stiffness. The latter is the result of self-healing, i.e. the hardening of the released epoxy resin.

The microscopic phenomena accompanying self-healing are revealed in Fig. 5 in the SEM images of the sample surface fractured by crack propagation. In the left-hand-side panel in Fig. 5, it is seen that the fractured PDMS surface looks like a brick wall near the panel bottom. However, in the middle of the sample zoomed-in in

the right-hand-side panel, several irregular epoxy chunks released from the fractured nanofibers are clearly visible.

In situ observations of the time-dependent solidification process of the epoxy resin in contact with the hardener released from the nanofibers damaged by a propagating crack are extremely challenging in the present samples. However, they are greatly facilitated by a macroscopic model experiments described in the Appendix.

4. Conclusion

Self-healing of composites with solution-blown nanofibers containing resin or hardener in the cores embedded in a PDMS matrix is possible. After rupture in the preliminary stretching, the tested nanofiber-containing composites could restore or even increase their stiffness (Young's modulus). The mechanism of self-healing is triggered by nanofiber rupture, the release of the epoxy resin and hardener (both viscous liquids), binary diffusion mixing of these epoxy components, and the curing reaction between them. The epoxy solidifies and seals over the broken links and/or crack tips, preventing further propagation of cracks. The control samples, which were the composites containing nanofibers without resin and hardener, revealed no self-healing. The self-healing effect was not observed at low damage levels or low strain levels, but was highly beneficial at moderate damage levels caused by moderate strains. However, the self-healing effect cannot save samples that reach the critical level of strain corresponding to catastrophic failure.

Acknowledgement

This work was supported by the International Collaboration Program funded by the Agency for Defense Development.

Appendix

1. Macroscopic view of epoxy release and hardening

To visualize the intrinsic mechanism of crack healing by the release of the epoxy resin and hardener, the following macroscopic test was conducted. A channel with the dimensions of 63 mm × 5 mm × 3.2 mm ($l \times w \times t$) was cast on a PDMS substrate, leaving the top surface open to the air. Two drops of ~0.3 mL in volume, one of the epoxy resin and the other of the hardener, were gently placed at the right and left ends of the channel, respectively. The hardener and the resin then spread from each side of the channel and made contact in the middle of the channel. The overlapping zone is located between the two vertical marks in the inset of Fig. A1. Photographs taken at regular time intervals allow the measurement of the mixing rate of the hardener and resin. The experimental data in Fig. A1 shows the increase in the width of the mixing zone (the latter manifests itself by a surface texture with ripples). If one assumes that mutual diffusion is responsible for the initial stage of the mixing process, the width of the mixing zone depends on time t as $x = const\sqrt{Dt}$, where D is the binary diffusion coefficient. Taking for the estimate $const \approx 1$, the diffusion coefficient D is evaluated as 1.556×10^{-5} cm^2/s. However, this fits the experimental data only up to $t = 3$ h, with $R^2 = 0.9674$. For larger values of t, the epoxy-hardening reaction affects the mixing zone, which solidifies and thereby arrests further binary diffusion while the propagation of the reaction front becomes saturated.

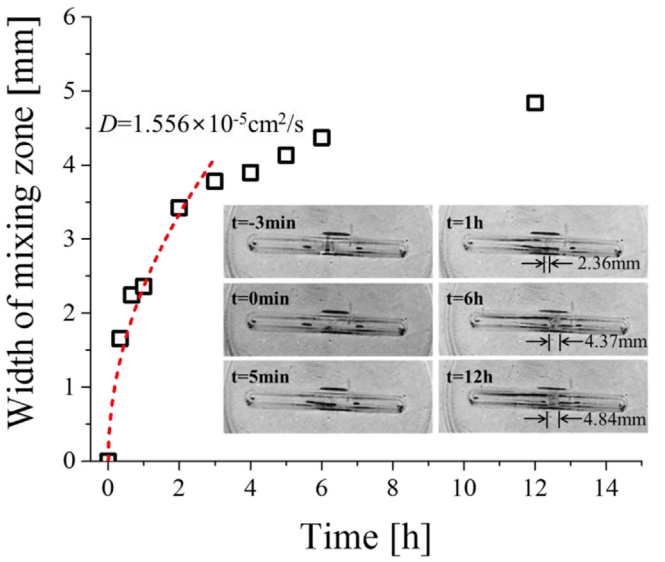

Fig. A1. Mixing of the two components, the epoxy resin (left) and the hardener (right). The experimentally measured width of the mixing zone is denoted in the images and depicted by symbols. Its fit with the curve $x = \sqrt{Dt}$ is shown by the dashed line.

2. Epoxy-hardener reaction observed in a macroscopic crack-tip-shaped mold

For a better understanding of the hardening process of the two parts of the epoxy, the reaction of the resin and the hardener in a crack-tip-like macroscopic mold was observed. Initially, the crack-like template was formed from polylactic acid (PLA) using a 3D printer (FlashForge Creator Pro), shown as the purple template in Fig. A2. This template was placed in a PDMS mold and left for 24 h. On removing the template, a macroscopic crack-like domain was cast in the PDMS body (Fig. A2).

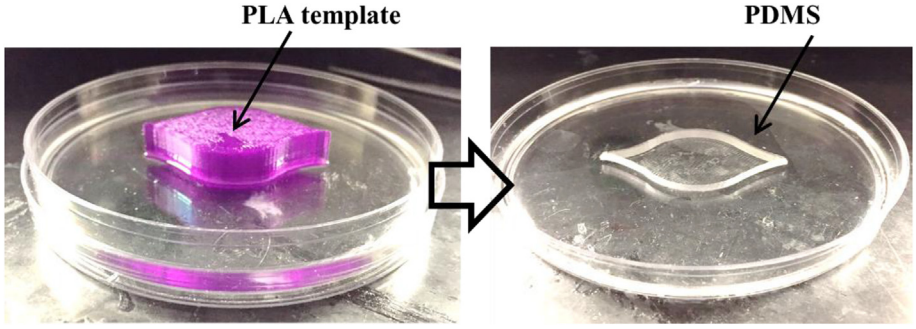

Fig. A2. 3D-printed PLA template shaped as a crack pressed into PDMS mold. Macroscopic crack-like domain formed in PDMS.

Two needles (25G with inner diameters of 0.25 mm and outer diameters of 0.51 mm) were inserted, with the needle tips placed at the boundary of the model crack of the solidified PDMS domain (Fig. A3). The two needles delivered the epoxy resin and its hardener separately. The dark resin and bright hardener are seen in Fig. A3. The viscosity of the hardener reported by the manufacturer in the Material Safety Data Sheet (MSDS) was 400 mPa s at 25 °C. The exact value of the epoxy resin viscosity was unavailable in literature. In the present work it was measured using the squeezing apparatus [21]. The measured viscosity of resin was 8.1 ± 0.9 mPa s at 25 °C. The resin and the hardener were supplied through the needles into the bottom left and top left sides of the model crack tip, respectively, using two separate syringe pumps at a flow rate of 1 mL/h. The syringe pumps were operated for ~10 min, with the total volumes of the supplied resin and hardener being ~160 μL each. The uncured resin and hardener appear to be smoothly spread along the rim of the crack from the tips of their respective needles (Fig. A3). After 2 h, both the epoxy and hardener stop spreading and a part of the cured epoxy is visible as a textured material in the photograph at $t = 6.5$ h in Fig. A3.

In the composites used in the present experiments, the diameters of the as-spun fibers containing the resin and hardener, which are embedded in a PDMS matrix, are ~200–1400 nm. Hence, the volume of the epoxy components released by the rupture of these fibers during tensile tests is much smaller than that used in the model crack experiment (Fig. A3). In the case of such nanofibers, tiny drops of both resin and hardener are released at the ruptured fiber tips and spread over the ruptured areas. The cured epoxy covering such ruptured nanofiber tips were visible in the SEM images of the cut nanofiber mats in our previous work (Fig. 4 there) [14]. To mimic this observed healing process at the crack tip, drops of the epoxy resin were positioned in a model crack tip and an excess of the hardener was supplied, as shown in Fig. A4. This caused strictly stoichiometric amounts of the resin and hardener to react at the crack tip. Then, curing occurred along the tip rim, as seen in Fig. A4, where the cured epoxy is seen as black dots in the panel corresponding to $t = 6.5$ h.

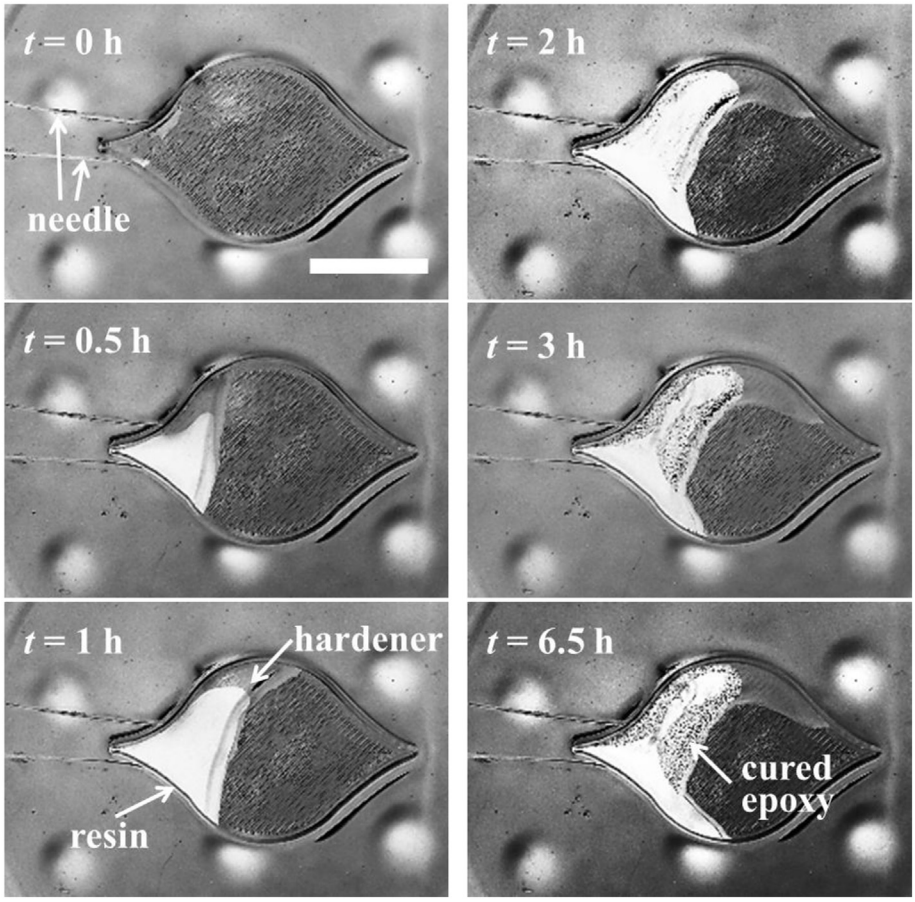

Fig. A3. Spreading and reaction of the epoxy resin and hardener released near the tip of the model crack. (Scale bar is 20 mm).

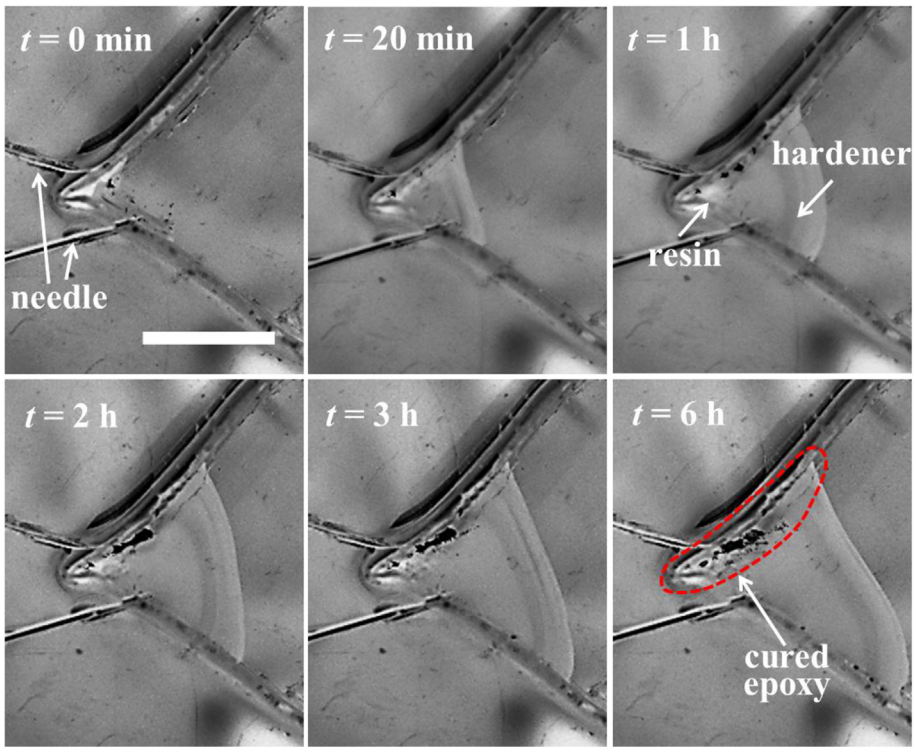

Fig. A4. Curing of a drop of the epoxy resin with an excess hardener at the tip of the model crack. (Scale bar is 10 mm).

References

[1] S.R. White, N.R. Sottos, P.H. Geubelle, J.S. Moore, M.R. Kessler, S.R. Sriram, E.N. Brown, S. Viswanathan, Autonomic healing of polymer composites, Nature 409 (2001) 794–797.
[2] K.S. Toohey, N.R. Sottos, J.A. Lewis, J.S. Moore, S.R. White, Self-healing materials with microvascular networks, Nat. Mater. 6 (2007) 581–585.
[3] K.S. Toohey, C.J. Hansen, J.A. Lewis, S.R. White, N.R. Sottos, Delivery of two-part self-healing chemistry via microvascular networks, Adv. Mater. 19 (2009) 1399–1405.
[4] C.J. Hansen, W. Wu, K.S. Toohey, N.R. Sottos, S.R. White, J.A. Lewis, Self-healing materials with interpenetrating microvascular networks, Adv. Mater. 21 (2009) 4143–4147.
[5] X.-F. Wu, A. Rahman, Z. Zhou, D.D. Pelot, S. Sinha-Ray, B. Chen, S. Payne, A.L. Yarin, Electrospinning core-shell nanofibers for interfacial toughening and self-healing of carbon-fiber/epoxy composites, J. Appl. Polym. Sci. 129 (3) (2012) 1383–1393.
[6] T.S. Coope, D.F. Wass, R.S. Trask, I.P. Bond, Metal triflates as catalytic curing agents in self-healing fibre reinforced polymer composite materials, Macromol. Mater. Eng. 299 (2014) 208–218.
[7] J.F. Patrick, K.R. Hart, B.P. Krull, C.E. Diesendruck, J.S. Moore, S.R. White, N.R. Sottos, Continuous self-healing life cycle in vascularized structural composites, Adv. Mater. 26 (25) (2014) 4302–4308.
[8] S. Sinha-Ray, D.D. Pelot, Z.P. Zhou, A. Rahman, X.-F. Wu, A.L. Yarin, Encapsulation of self-healing materials by coelectrospinning, emulsion electrospinning, solution blowing and intercalation, J. Mater. Chem. 22 (2012) 9138–9146.
[9] X.-F. Wu, A.L. Yarin, Recent progress in interfacial toughening and damage self-healing of polymer composites based on electrospun and solution-blown nanofibers: an overview, J. Appl. Polym. Sci. 129 (2013) 2225–2237.
[10] S. Goldsmith, Southwest Airlines Flight 2294 Lands in West Virginia with Football-sized Hole in Fuselage, 2009. http://www.nydailynews.com/news/world/southwest-airlines-flight-2294-lands-west-virginia-football-sized-hole-fuselage-article-1.397715.
[11] M.W. Lee, S. An, H.S. Jo, S.S. Yoon, A.L. Yarin, Self-healing nanofiber-reinforced polymer composites: 1. Tensile testing and recovery of mechanical properties, ACS Appl. Mater. Interfaces 7 (2015) 19546–19554.
[12] A. Das, A. Sallat, F. Bohme, M. Suckow, D. Basu, S. Wießner, K.W. Stockelhuber, B. Voit, G. Heinrich, Ionic modification turns commercial rubber into a self-healing material, ACS Appl. Mater. Interfaces 7 (2015) 20623–20630.
[13] M.W. Lee, S. An, H.S. Jo, S.S. Yoon, A.L. Yarin, Self-healing nanofiber-reinforced polymer composites: 2. Delamination/debonding, and adhesive and cohesive properties, ACS Appl. Mater. Interfaces 7 (2015) 19555–19561.
[14] M.W. Lee, S.S. Yoon, A.L. Yarin, Solution-blown core–shell self-healing nano- and microfibers, ACS Appl. Mater. Interfaces 8 (2016) 4955–4962.
[15] M.W. Lee, S. An, C. Lee, M. Liou, A.L. Yarin, S.S. Yoon, Self-healing transparent core-shell nanofiber coatings for anti-corrosive protection, J. Mater. Chem. A 2 (19) (2014) 7045–7053.
[16] S. An, M. Liou, K.Y. Song, H.S. Jo, M.W. Lee, S.S. Al-Deyab, A.L. Yarin, S.S. Yoon, Highly flexible transparent self-healing composite based on electrospun core-shell nanofibers produced by coaxial electrospinning for anti-corrosion and electrical insulation, Nanoscale 7 (2015) 17778–17785.
[17] S.H. Cho, S.R. White, P.V. Braun, Self-healing polymer coatings, Adv. Mater. 21 (2009) 645–649.
[18] M.W. Lee, S. Sett, S.S. Yoon, A.L. Yarin, Fatigue of self-healing nanofiber-based composites: static test and subcritical crack propagation, ACS Appl. Mater. Interfaces 8 (2016) 18462–18470.
[19] G.I. Barenblatt, Flow, Deformation, and Fracture, Cambridge University Press, Cambridge, 2014.
[20] G. Cherepanov, Mechanics of Brittle Fracture, McGraw Hill, New York, 1979.
[21] D.D. Pelot, R.P. Sahu, S. Sinha-Ray, A.L. Yarin, Strong squeeze flows of yield-stress fluids: the effect of normal deviatoric stresses, J. Rheol. 57 (2013) 719–742.